TÜBİTAK

Turkish Journal of Earth Sciences

http://journals.tubitak.gov.tr/earth/

Research Article

Turkish J Earth Sci
(2016) 25: 64-80

doi:10.3906/yer-1504-17

Tracking the uplift of the Bolkar Mountains (south-central Turkey): evidence from apatite fission track thermochronology

Fatih KARAOĞLAN*
Department of Geological Engineering, Faculty of Engineering and Architecture, Çukurova University, Balcalı-Sarıçam, Adana, Turkey

Received: 15.04.2015 • **Accepted/Published Online:** 23.11.2015 • **Final Version:** 01.01.2016

Abstract: Apatite fission track (AFT) thermochronology is applied to the Horozköy granitoid, which outcrops within the Bolkar Mountains (south-central Turkey). The region comprises the Niğde Massif to the north, the Inner Tauride Suture Zone, and the Central Taurides to the south. The Niğde Massif and the Central Taurides collided during the Eocene following north-dipping subduction of the Inner Tauride Ocean beneath the Niğde Massif. The Ulukışla Basin formed above this suture zone. The AFT ages range between 23 and 16 Ma, although there was no significant uplift or exhumation during this period. During the Oligo-Miocene, the region experienced a slow uplift and the collapse of the Tauride belt, in response to the mantle processes (roll-back, break-off, and/or slab tearing) related to the African plate and linked oceanic slab beneath the Anatolide-Taurides. The Central Taurides reached maximum height during the latest Miocene. The AFT modeling results indicate a fast exhumation in the late Miocene-Pleistocene, consistent with the biostratigraphic and field evidence.

Key words: Central Taurides, Bolkar Mountains, Horozköy granitoid, apatite fission track, exhumation, uplift

1. Introduction

South-central Anatolia hosts two major units, namely the Central Anatolian Crystalline Complex (CACC) to the north and the Central Taurides to the south. The Bolkar Mountains, part of the Central Taurides, which are bounded by the Ecemiş Fault to the east and the Kırkkavak Fault to the west (Blumenthal, 1960; Özgül, 1984), and the CACC juxtaposed following the subduction of the Inner Tauride Ocean during the Late Cretaceous-Eocene (Görür et al., 1984; Dilek et al., 1999a; Clark and Robertson, 2002; Pourteau, 2011; Robertson et al., 2012; Parlak et al., 2013; Sarıfakıoğlu et al., 2013; Pourteau et al., 2014). The collision between the Arabian platform and the Taurides occurred during the Oligocene-Miocene, resulting in shortening, thickening, and uplifting in east Anatolia and westward extrusion of central and western Anatolia. Thus, the Central and Eastern Anatolian plateaus span a transition from crustal shortening in the east to westward block extrusion and extension, accommodated mostly along the North and East Anatolian faults (Şengör and Yılmaz, 1981; Şengör et al., 1985; Yılmaz, 1993; Yılmaz et al., 2007; Okay et al., 2010; Elitok and Dolmaz, 2011; Schildgen et al., 2014; Karaoğlan et al., 2015). The thickened crust reaches as high as 3–3.5 km above sea level in east and central Anatolia along the suture zones, where the Central Anatolian Plateau reaches elevations of about 500–1500 m (Tezel et al., 2013). The westward escape of Anatolia compounded the convergence and collision with the Afro-Arabian plate along the Bitlis-Zagros Suture Zone (Dewey et al., 1986; Jolivet and Faccenna, 2000; McClusky et al., 2000; Robertson and Mountrakis, 2006; Smith, 2006; Allen and Armstrong, 2008; Ring et al., 2010; Elitok and Dolmaz, 2011; van Hunen and Allen, 2011) (Figure 1).

The exhumation of the CACC exhibits distinct features at its margins. The exhumation of the northern part of central Anatolia was related to the collision of Eurasia and Anatolia during the early-middle Paleocene, while the eastern part of the CACC was exhumed as a result of the Tauride-Arabia collision during the Oligocene (Boztuğ and Jonckheere, 2007). The fission-track data suggest that the southern margin of central Anatolia, linked with Central Taurides, was exhumed at 17–11 Ma in a yo-yo tectonic regime (Fayon and Whitney, 2007; Umhoefer et al., 2007; Whitney et al., 2008).

South-central Anatolia first emerged above sea level during the Eocene, where the southern flank of the Taurides

* Correspondence: fkaraoglan@cu.edu.tr

still remained under sea level (Aksu et al., 2005a; Jaffey and Robertson, 2005). The emergence of the Bolkar Mountains was a part of the regional south-central Anatolian uplift, as a result of complex mantle processes (subduction roll-back, slab break-off, slab tearing) that resulted from the north-dipping southern branch of the Neo-Tethys Ocean beneath the Anatolide-Tauride continent during the Oligo-Miocene (Barazangi et al., 2006; Dilek and Sandvol, 2009; van Hinsbergen et al., 2009; Ring et al., 2010; Biryol et al., 2011; van Hunen and Allen, 2011; Cosentino et al., 2012; Schildgen et al., 2012a, 2012b, 2014). The uplift of the Bolkar Mountains within the Central Taurides shows temporal discrepancies against the exhumation of the CACC. The Bolkar Mountains appear to have been exhumed slightly earlier then the CACC during the late Eocene-early Miocene (Dilek et al., 1999b; Lefebvre et al., 2015). The available low-temperature thermochronologic data suggest that the uplifting is propagated from south to north or the paleogeothermal gradient was located at a higher position in the south, where the Central Taurides were already at maximum height during the Oligocene-Miocene (Dilek et al., 1999b; Fayon and Whitney, 2007; Umhoefer et al., 2007; Lefebvre et al., 2015). During the late Miocene-Pleistocene, the crustal uplift rate changed and the late Miocene marine sediments uplifted up to 1.5–2 km (Schildgen et al., 2012a, 2012b). The field, biostratigraphic, and cosmogenic dating data from CACC and the Central Taurides suggest that the continuing slab break-off and/or slab tearing led to the fast uplifting of south-central Anatolia and emergence above sea level starting at ~7 Ma ago (Cosentino et al., 2012; Schildgen et al., 2012a, 2012b). Recent studies show that the Arabia-Africa and Eurasia collision was responsible for the Oligocene-early Miocene exhumation and/or uplifting, whereas the mantle processes beneath south-central Anatolia were responsible for the high uplift rates within the CACC and Central Taurides (Cosentino et al., 2012; Schildgen et al., 2012a, 2014; Cipollari et al., 2013; Radeff et al., 2015). The latest Miocene-Recent uplifting of the Central Taurides and CACC is well documented (Cosentino et al., 2012; Schildgen et al., 2012a, 2014; Yildirim et al., 2013; Radeff et al., 2015); however, the Oligocene-early Miocene history is still under debate in the frame of timing of exhumation and the effect of subduction and collisional events on the Central Taurides.

In this study, apatite fission track (AFT) thermochronology is applied to a postcollisional granitoid, the so-called adakitic Horozköy granitoid, that intruded into the Bolkardağ Units (Central Taurides) during the early-middle Eocene. This paper discusses the thermochronologic (AFT) evidence related to the exhumation and uplift of the Bolkar Mountains, located to the north of the easternmost Mediterranean Sea (Figure 1), and the relation between the exhumation/uplifting and the mantle processes.

2. General geology

South-central Anatolia comprises two main tectonic units separated by the Inner Tauride Ocean and the CACC to the north and the Central Taurides to the south, where the Ulukışla Basin formed (Demirtaşlı et al., 1984; Görür et al., 1984; Dilek et al., 1999a) (Figure 1). The CACC, first described by Göncüoğlu et al. (1991), was formed by three metamorphic units, namely the Kırşehir, Akdağ, and Niğde massifs, distinguished by their metamorphism. The Kırşehir and Akdağ massifs experienced clockwise P/T paths at moderate P/T conditions, with upper amphibolite (highest) overprint, whereas the Niğde Massif underwent two distinct metamorphisms between the Late Cretaceous (Göncüoğlu, 1986; Whitney and Dilek, 1997; Whitney et al., 2007) and early-middle Cenozoic (Whitney and Dilek, 1997, 1998, 2000; Fayon et al., 2001; Whitney et al., 2001; Dilek and Sandvol, 2009).

The Inner Tauride Suture Zone (ITSZ), bounding the southern margin of the CACC, was formed by the consuming of the Inner Tauride Ocean in a north-dipping subduction beneath the CACC during the Late Cretaceous-early Cenozoic (Dilek et al., 1999a; Okay and Tüysüz, 1999; Parlak and Robertson, 2004; Robertson, 2004; Kadıoğlu et al., 2006; Kadıoğlu and Dilek, 2010; Pourteau et al., 2010, 2013; Parlak et al., 2013; Sarıfakıoğlu et al., 2013). During Paleocene (Late Cretaceous?) and Miocene time, above the ITSZ, the Ulukışla Basin formed in an E-W trending seaway. The Ulukışla Basin contains marine and terrestrial sedimentary rocks, evaporites, volcanosedimentary rocks, and volcanic and intrusive magmatic units with a thickness of up to 5 km (Demirtaşlı et al., 1973, 1984; Clark and Robertson, 2002, 2005; Kurt et al., 2008; Engin, 2013) (Figure 1). To the south, the basal units of the basin composed of conglomerates, calcarenite, and limestone unconformably rest on the Central Taurides, represented by the Bolkardağ Unit (Figure 2).

The Bolkardağ Unit, to the south of the CACC, comprises carbonate, siliciclastic, and volcanic rocks and their metamorphic equivalents with ages ranging from Upper Permian to Late Cretaceous (Demirtaşlı et al., 1973, 1984; Özgül, 1976). This unit is interpreted as a ribbon-shaped continent rifted off from Gondwana (Özgül, 1976, 1984; Robertson and Dixon, 1984; Görür et al., 1991; Garfunkel, 1998, 2004). The Bolkardağ Unit (Bolkar Group of Demirtaşlı et al., 1984) may be divided into four formations: 1) the Dedeköy formation (Permian), 2) Gerdekesyayla formation (Lower-Middle Triassic), 3) Berendi limestone (Upper Triassic), and 4) Üçtepeler limestone (Jurassic-Cretaceous) (Demirtaşlı et al., 1973, 1984). The lowermost part of the Bolkardağ Unit begins

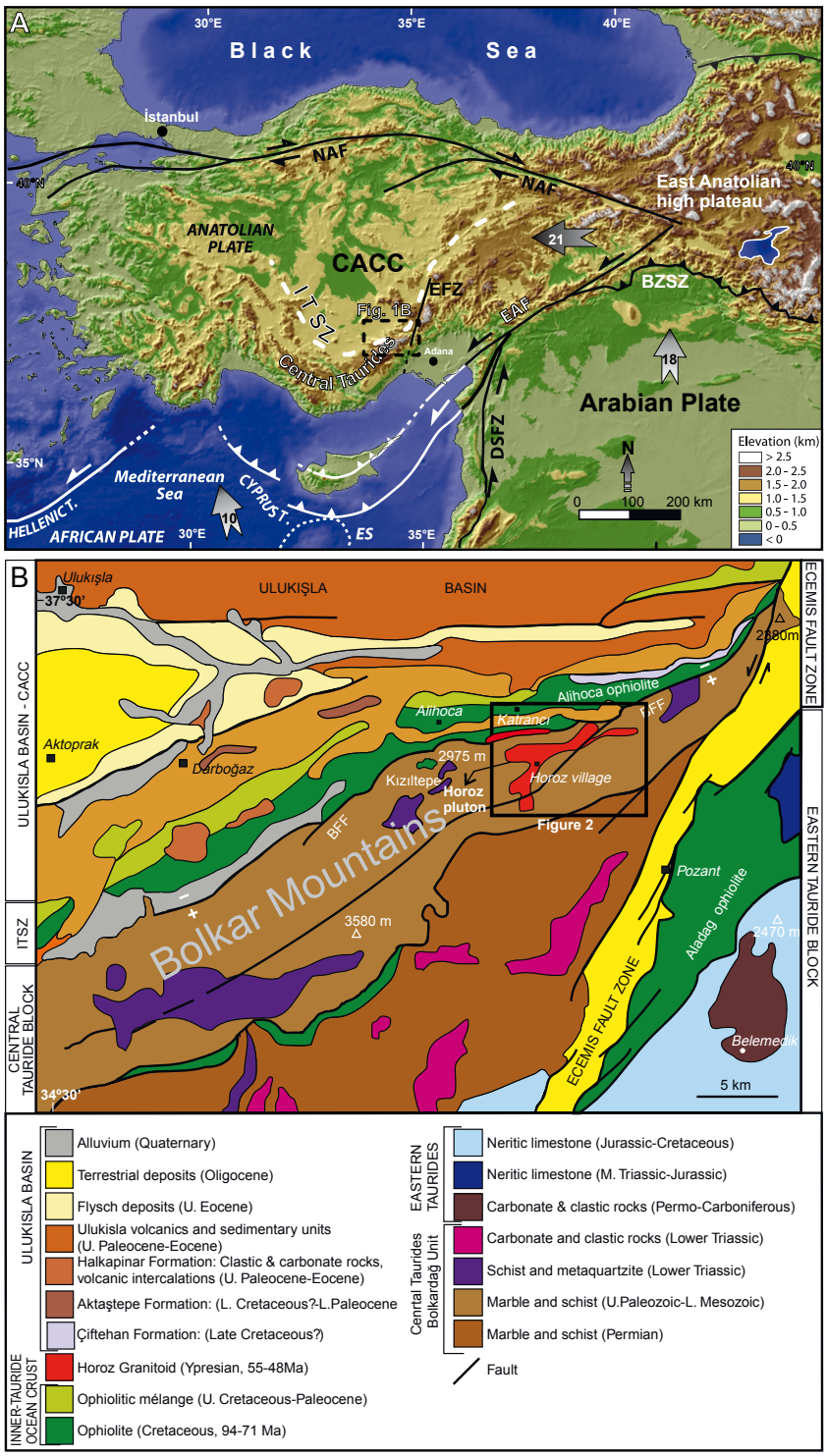

Figure 1. A) Regional topography map (SRTM V4.1 data from Jarvis et al. (2008) showing major tectonic boundaries. CACC: Central Anatolian Crystalline Complex; CP: Central Pontides; BZSZ: Bitlis-Zagros suture zone; NAF: North Anatolian Fault; EAF: East Anatolian Fault; DSFZ: Dead Sea Fault Zone; EFZ: Ecemiş Fault Zone; ES: Eratosthenes Seamount; LV: Lake Van. Arrows with numbers inside represent plate movement (mm/year) with respect to Eurasia (Reilinger et al., 1997); map modified after Schildgen et al. (2014). B) Geological map of south-central Turkey. Data from Clark and Robertson (2002), Dilek and Sandvol (2009), and Engin (2013).

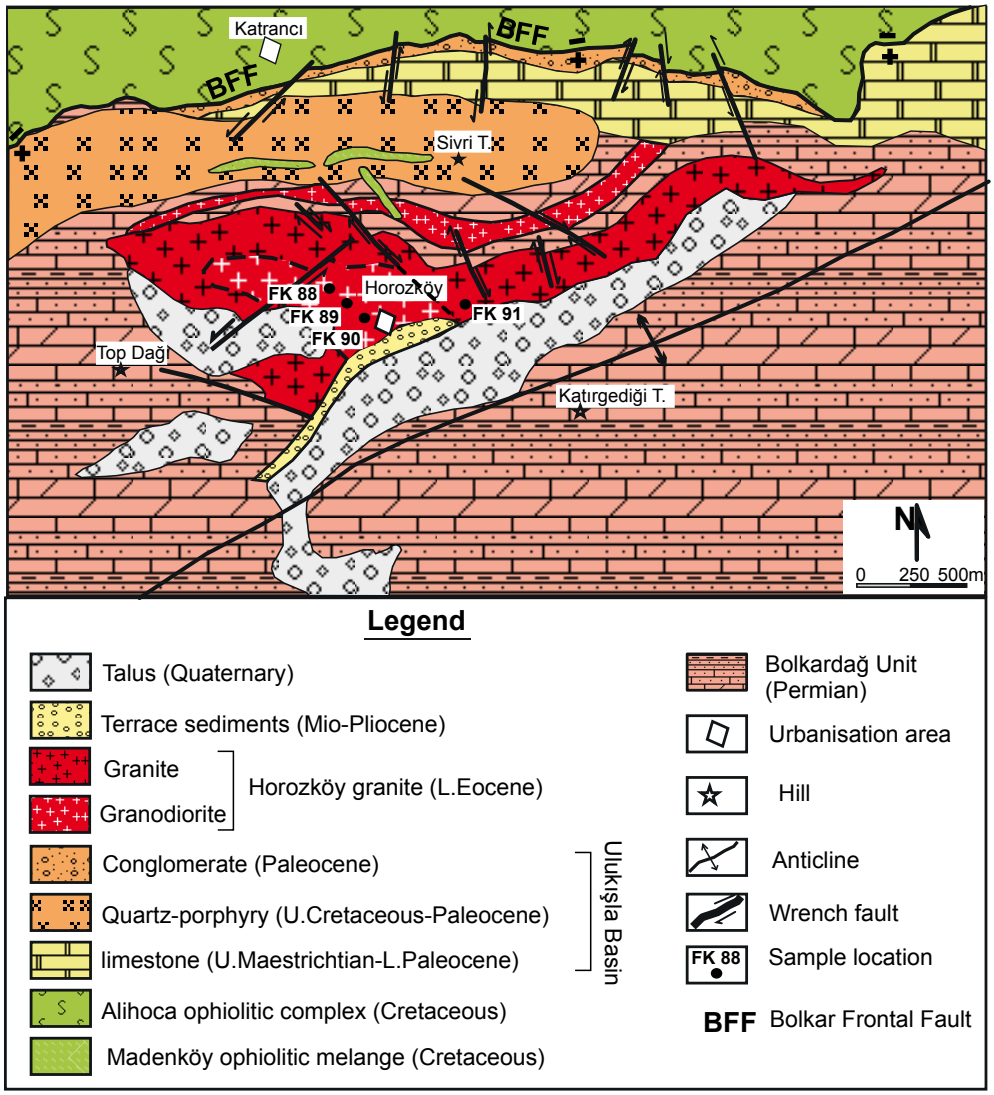

Figure 2. Geological map of Horoz village and surroundings (modified after Çalapkulu, 1980; Çevikbaş et al., 1995; Kadıoğlu and Dilek, 2010; Kocak et al., 2011).

with dolomitic limestones intercalated with micaceous slates (Dedeköy formation-Upper Permian). The Dedeköy formation formed under stable shelf conditions and has a thickness of 600 m. Upwards, this unit passes into shale and clayey limestone alternation continued with limestone, thick-bedded dolomitic limestone, and shale and clayey limestone alternation named as the Gerdekesyayla formation, which was formed in an open marine shelf during the Lower-Middle Triassic. The upper part of the Bolkardağ Unit is predominantly represented by a thick carbonate sequence including dolomite, fine-grained limestone, and medium to thick-bedded dolomitic limestone, formed in a shallow marine, stable carbonate platform during the Upper Triassic (Berendi limestone). Upwards, the Berendi limestone passes into partly oolitic and dolomitic limestone, dolomite, and limestone (Üçtepeler limestone). The formation formed in an open marine and deep pelagic sedimentary environment during the Jurassic-Late Cretaceous (Demirtaşlı et al., 1973, 1984). The Gerdekasyayla formation shows greenschist metamorphism, whereas biotite, tourmaline, and almandine crystals are formed near the contact zones of the Horozköy granitoid (Çalapkulu, 1980). The dykes of the Horozköy granitoid intruded into the marbles (Çalapkulu, 1980; Çevikbaş et al., 1995).

The Central Tauride block (including the Bolkardağ Unit) was shortened and thickened as a result of folding and imbrication along the thrust faults such as the Bolkar Frontal Fault (Demirtaşlı et al., 1984; Dilek et al., 1999b). The obduction of oceanic lithosphere (i.e. Alihoca

ophiolite) from the north and continuous subduction of the northern edge of the Central Taurides (Dilek and Whitney, 1997; Dilek and Flower, 2003; Dilek and Sandvol, 2009) was responsible for the shortening and thickening of the Paleozoic-Jurassic tectonostratigraphic units in the Tauride block during the Late Cretaceous and Eocene (Dilek et al., 1999b; Dilek and Sandvol, 2009; Parlak et al., 2013, 2014). The isostatic rebound of the partially subducted continent, as a result of the subduction processes, caused the northern edge of the entire Tauride block to be gradually uplifted along the normal faults (i.e. the Bolkar Frontal Fault) during the Miocene, building a southward-tilted asymmetric mega-fault block with a rugged, alpine topography (Dilek and Whitney, 1997, 2000; Dilek et al., 1999b; Dilek and Sandvol, 2009; Kadıoğlu and Dilek, 2010) (Figures 1 and 2). In the study area, the Bolkardağ Unit forms a big anticlinorium, where most of the anticlines are asymmetrical and overturned towards the north along the Bolkar Frontal Fault (Demirtaşlı et al., 1984) (Figure 2). The Bolkar Frontal Fault has an ENE-trending left-lateral oblique-slip component and displays a top-to-the-north shear sense indicator. The fault system has multiple splays within the northern edge of the Tauride block and is defined by mylonitic breccia composed of ophiolitic and carbonate rocks (Dilek and Whitney, 2000). The structural trend of the normal faults is generally ENE-WSW in the study area (Figure 2).

The fluvial terrace unit, observed in the Horoz valley, is slightly tilted to downslope. This unit rests on the Horozköy granitoid and seals the normal faults along the valley, containing mainly marble and granitoid pebbles and blocks with up to 250 m in thickness. The age of the terrace unit was reported as Oligocene by Çalapkulu (1980); however, Dilek et al. (1999b) proposed a Mio-Pliocene age for the unit.

2.1. Horozköy granitoid

The Horozköy granitoid outcrops in an area of ~8 km^2 within the Bolkardağ region in the eastern part of the Central Taurides, where it took the name of the Horoz village (Figure 2). The granitoid body intruded into the northern flank of a NE-SW trending anticline including the Lower Marble unit and the schists of the Bolkardağ unit, whereas a Plio-Quaternary terrace unit overlies the southern part. The granitoid, first described by Blumenthal (1956), has a contact metamorphic aureole represented by hornblende hornfels and garnet fels facies rocks. The tonalite and diorite dykes intruded into the wall rocks (Demirtaşlı et al., 1973, 1984; Çalapkulu, 1980; Çevikbaş and Öztunalı, 1992; Çevikbaş et al., 1995; Kadıoğlu and Dilek, 2010). Engin (2013) reported that the dykes of the Horozköy also intruded into the Eocene Ulukışla Basin units. The unit is composed of two parageneses: the granite is composed of quartz, plagioclase, K-feldspar, biotite, and hornblende, and the granodiorite is composed of quartz, feldspar, biotite, and amphibole (Çalapkulu, 1980; Çevikbaş et al., 1995; Kadıoğlu and Dilek, 2010). Both rock types are intruded by mafic and felsic dykes and include mafic microgranular enclaves, indicating that magma mixing/mingling processes played an important role during crystallization (Kadıoğlu and Dilek, 2010; Kocak et al., 2011).

The Horozköy granitoid rocks were interpreted to have formed in a postcollisional extensional environment as a result of the collision of the Central Taurides with the CACC (Kadıoğlu and Dilek, 2010). The earlier suggestions for the formation (crystallization) age of the Horozköy granitoid were based on cross-cutting relationships with the Cretaceous ophiolitic mélange that rests tectonically on the Bolkardağ marbles, reported to be post-Lower Paleocene to pre-Lower Eocene (Çalapkulu, 1980) and pre-Paleocene or Late Cretaceous-Paleocene (Çevikbaş and Öztunalı, 1992). Zircon U-Pb dates indicate a slightly younger formation age, ranging from 56 to 48 Ma (Dilek et al., 1999b; Kadıoğlu and Dilek, 2010; Kuscu et al., 2010; Engin, 2013; Parlak et al., 2013), whereas the ^{40}Ar-^{39}Ar cooling ages (hornblende, 47 Ma, and biotite, 54–50 Ma) yield a similar age range (Kuscu et al., 2010). Dilek et al. (1999b) also reported an AFT age of 23.6 ± 1.2 Ma, suggesting that the granitoid uplifted during the Miocene. The undeformed Mio-Pliocene fluvial terrace unit within the incised valley indicates that the Central Taurides were already uplifted during this period (Dilek et al., 1999b).

3. Analytical procedure

Four samples were taken from the fresh outcrops across a range of altitudes to illustrate the exhumation rate (Table 1). The mineral separation procedures including crushing, sieving, wet sieving, electromagnetic, and heavy liquid techniques were performed in the Çukurova University Geological Engineering Department (Adana, Turkey). The samples were mounted in epoxy resin, ground, and polished prior to etching. The samples were etched in 5.5 M HNO_3 medium for 20 s at 21 °C (Donelick et al., 1999). The mounts were covered with 50-mm uranium-free muscovite external detectors and irradiated in a BR-1 research reactor in Belgium. Three age standards including the IRMM 540R uranium glass and the c-axis oriented Durango apatites, prepared in the same manner as the samples, were included in the irradiation can in order to ensure that the tracks were counted in the same faces in the standard as in the samples and to guarantee minimum separation between the standard glasses and apatite age standard to avoid possible radial fluence gradients for minimizing the systematic error of individual z values (Table 2). To calculate the neutron flux, a 1% Al-Co-monitor (IRMM-528R) of 0.01 mm in thickness was

Table 1. Apatite fission track analytical data for Horozköy granitoid.

Sample	Elevation (m)	Irradiation step	Grains	$\rho_s \pm 1\sigma$	N_s	$\rho_i \pm 1\sigma$	N_i	$P(\chi^2)$	$\rho_d \pm 1\sigma$	N_d	ξ Age ± 1σ (Ma)	Number of lengths	Mean track length	Stand. dev.
FK 88	1318	FG-65	33	17.94 ± 1.56	592	51.00 ± 4.66	1683	30.70	0.505 ± 0.008	4535	23.7 ± 1.3	82	14.80	2.15
FK 89	1188	FG-65	42	15.98 ± 1.58	670	53.52 ± 5.86	2918	24.85	0.515 ± 0.008	4664	20.5 ± 1.0	78	17.19	4.58
FK 90	1130	FG-65	14	7.86 ± 0.80	110	33.86 ± 5.44	474	59.01	0.520 ± 0.007	4790	16.1 ± 1.7	8	16.25	5.97
FK 91	1080	FG-65	46	8.00 ± 0.59	368	28.89 ± 1.99	1329	65.88	0.525 ± 0.007	4892	19.4 ± 1.2	55	17.17	4.81

N: Numbers of tracks counted; Analyses by external detector method using 0.5 for the 4π/2π geometry correction factor (Gleadow and Lovering, 1977); ages calculated using dosimeter glass IRMM-540R; (apatite) ξ IRMM540R = 267 ± 5 (see Table 2); $P(\chi^2)$ is probability of obtaining χ^2 value for v degrees of freedom, where v = number of crystals-1; ξ age is a modal age, weighted for different precisions of individual crystals (Galbraith and Laslett, 1993).

Table 2. ξ calibration calculations.

DUR	Irradiation	Standard	**ξ**	Error	$1/Error^2$	$ξ/Error^2$	**ρd** [10^6 cm^{-2}]	Error [ρ_D]	Z [Ma]	Error [Z]
	FG 65	DD 21	268.4	10.9	0.008	2.262	0.502	0.008	134.8	10.0
	FG 65	DD 22	266.0	8.0	0.016	4.188	0.533	0.008	141.6	6.8
	FG 65	DD 23	266.6	7.8	0.016	4.386	0.435	0.007	116.1	6.3
Mean [1s]	(unweighted)		267.0	0.7	0.041	10.836	0.490	0.029	130.8	7.6
Mean [1s]	(weighted)		266.7	5.0						

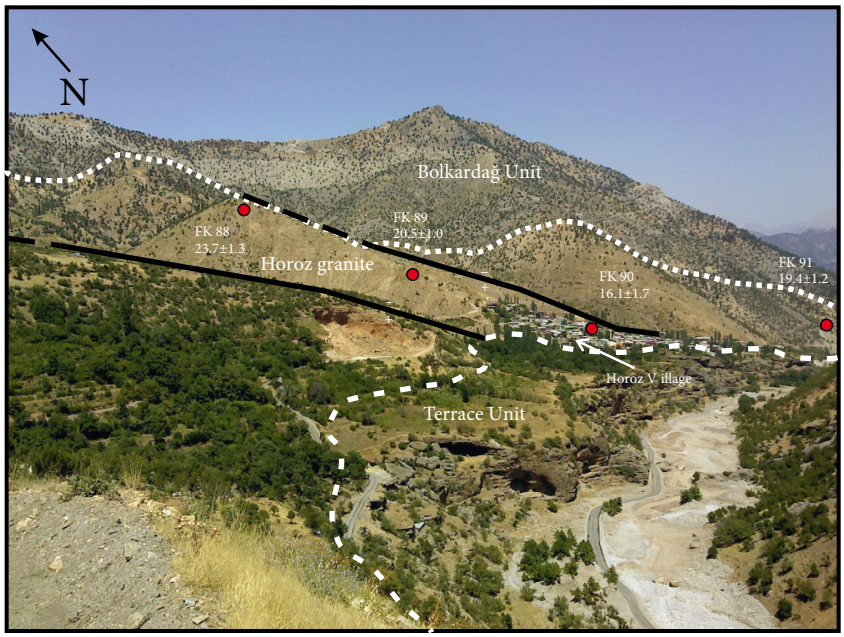

Figure 3. Field photo of the Horozköy granitoid near Horoz village including sample locations with AFT age data.

added above each standard in the irradiation can. After irradiation, the induced tracks in the external detectors were etched in 48% HF for 30 min.

The track counts were carried out in transmitted light at a magnification of 1250× with a Zeiss AxioImager microscope. The counting procedure of Jonckheere et al. (2003) was followed for counting. During the counting the external detectors were repositioned track-side down on the mounts, in the same position as during irradiation. The fossil tracks were counted by focusing on the apatite surface through the muscovite external detector, whereas the induced tracks were counted by focusing on the underside of the external detector, without moving the microscope stage. Three age standards were counted for the determination of the z calibration factor. At least 2500 fossil tracks were counted in the apatite, and over 3000 induced tracks in the muscovite external detector and 4000 tracks in the external detector irradiated against the uranium glass were counted. The calculation of the z calibration factors and the unweighted overall mean z are given in Table 2. Approximately 40 grains were counted in each sample (only in one sample 14 grains were counted) to ensure the total number of fossils and induced fission tracks were sufficient for reasonable ages. The results and the age calculations are given in Table 1.

The track length measurements were carried out with a Zeiss AxioImager microscope at a magnification of 2500× equipped with an Autoscan stage and a digitizer connected to a computer with Trakscan software. In order to reveal a sufficient number of confined tracks, the mounts were over-etched with the same medium as etching done at 15 s prior to measurements. Trackscan software allows users to measure not only horizontal but also oriented tracks. Between 50 and 100 confined tracks were measured in prismatic faces with the selection of only tracks in tracks (TINTs) (Table 1).

The track counts, track lengths with c-axis angles, and dpar values were used in the inverse modeling for calculating the thermal histories. The thermal histories were modeled with computer software HeFTy 1.8 (Ketcham, 2005). The annealing equations of Donelick et al. (1999) and c-axis projection of Donelick et al. (1999) were used during inverse modeling calculations. A minimum of 50,000 (at least 250 good paths) candidate temperature-time (T-t) paths were generated at random (Monte Carlo algorithm) for each modeling run.

4. Analytical results

The combined geo/thermochronologic data suggest a fast cooling through 300 °C (McDougall and Harrison, 1999) after emplacement, which can be explained by either shallow emplacement or fast exhumation above 10 km in depth for the Horozköy granitoid (Dilek et al., 1999b; Kuscu et al., 2010; Engin, 2013; Parlak et al., 2013). The single-grain fission track ages show very low dispersion and are consistently younger than the intrusion age of granitoid (Table 1; Figure 3). Samples were taken at different altitudes of the granitoid around Horoz village

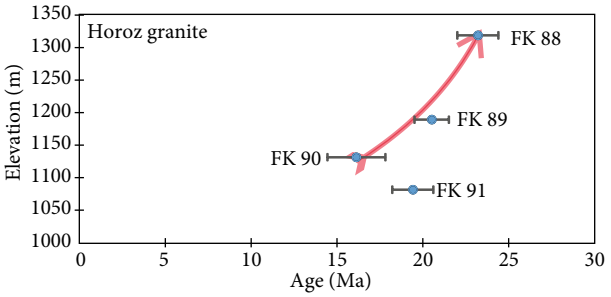

Figure 4. Age-elevation diagram of the AFT results. FK91 deviates from the normal trend as a result of faulting after exhumation.

(Figure 3) to detect the possible age-elevation profile. AFT ages range between 23.7 and 16.1 Ma, where the oldest AFT age is similar to the age reported by Dilek et al. (1999b) (Table 1; Figure 3). The ages show a clear correlation with elevation, except FK91, which is separated from the others by a normal fault in the field (Table 1; Figures 3 and 4).

To calculate the cooling or exhumation rate, one can perform either the mineral pair method, using one rock sample with multiple mineral cooling ages, or the altitude-dependence method, performing the same dating method on two (or more) samples from different altitudes. The latter requires no important vertical tectonic displacement during or after exhumation. If any tectonic activity occurred after the youngest isotopic age, then the linear relationship between altitude and age will be disrupted (Gallagher et al., 1998; Balestrieri et al., 2003; Gallagher et al., 2005). After excluding FK91, the age-elevation plot drawn with the ages obtained in this study indicates a slow exhumation (nearly steady) of ~0.03 mm/year for the Early Eocene-aged Horozköy granitoid between 23 and 16 Ma (Early Miocene) (Figures 3 and 4). The AFT age reported by Dilek et al. (1999b) cannot be used for the age-elevation profile, as the elevation data and the methodology of AFT age were not reported.

Three T-t paths were calculated using HeFTy computer software by inverse modeling to reconstruct the exhumation of the samples in the partial annealing zone (PAZ) (Ketcham, 2005). The number of track lengths within sample FK90 was insufficient to provide a statistically meaningful result. The T-t path of sample FK88, calculated by inverse modeling, indicated similar results with measured ages (Figure 5). The sample was cooled below 100 °C after 25 Ma and remained in the PAZ until 2–3 Ma (Figure 5). The probability of the chi-square test ($P(\chi^2)$ = 30.70) for this sample indicates a uniform age distribution between intergrains. The track length (TL) distribution of FK88 shows a unimodal distribution with a mean length of 14.80 µm and standard deviation of 2.15 µm (Table 1; Figure 5). The TL distribution implies a slow cooling rate in the PAZ, which is consistent with the age-elevation and cooling history. Sample FK89 was in the total annealing zone before 25 Ma and has a cooling history similar to that of FK88. The grains ages of FK89 are concordant ($P(\chi^2)$ = 24.85) and the confined TL shows a unimodal distribution, ranging between 10 and 17 µm with a mean length of 17.19 µm (Table 1). The very high standard deviation of the TL implies that the samples remained long enough in the PAZ to shorten the old tracks, which is consistent with the slow cooling suggested by the age-elevation profile. This sample spans a more or less steady uplift in the PAZ, cooled below ~90 °C slowly after 7–8 Ma, and afterward the cooling rate of the sample increased (Figure 5). The age of sample FK91 indicates that normal faulting was active after the early Miocene, when the samples had been exhumed above the PAZ. In contrast to this early Miocene cooling age, the T-t modeling based on track length data indicates a rapid undercooling from the PAZ to the total stability zone in a time span between 6 and 8 Ma (Figure 5) (Wagner and Van den Haute, 1992; Van Den Haute and De Corte, 1998).

5. Discussion

The accumulating low-temperature data from central and eastern Anatolia cluster into three groups (Dilek et al., 1999b; Fayon et al., 2001; Boztuğ and Jonckheere, 2007; Umhoefer et al., 2007; Boztuğ et al., 2008, 2009a, 2009b, 2009c; Okay et al., 2010; Karaoğlan, 2012; Karaoğlan et al., 2015). The oldest age group is Paleocene-Eocene from the granitoids, located to the northern edge of the CACC, related to the closure of the northern branch of the Neo-Tethys Ocean and the collision between Eurasia and the CACC (Boztuğ and Jonckheere, 2007; Boztuğ et al., 2008, 2009c), whereas there are also Oligocene cooling ages from the metamorphic rocks of the CACC (Fayon et al., 2001). The second age group is Eocene-Oligocene, related to the first collision of the Anatolide-Tauride platform and the Arabian platform, which is also related to the third and the youngest age group (Miocene) (Fayon and Whitney, 2007; Umhoefer et al., 2007; Okay et al., 2010; Karaoğlan et al., 2015) (Figure 6). According to the complexity of the collision events in the Anatolian peninsula, one must use these data with care. The previous fission-track data from south-central Anatolia indicate an Early-Late Miocene cooling/uplift for this region (Dilek et al., 1999b) (Figure 6). The Niğde Massif and the Tauride block collided following the subduction of the Inner Tauride Ocean during the Late Cretaceous-Eocene (Dilek and Whitney, 1997; Kadıoğlu and Dilek, 2010; Parlak et al., 2013). Following the deposition of the Ulukışla Basin above the suture zone, the Bolkar Mountains and the Ulukışla Basin remained under sea level, whereas high levels of the Niğde Massif emerged and eroded during the Eocene. During this stage the Ecemiş Fault activated and

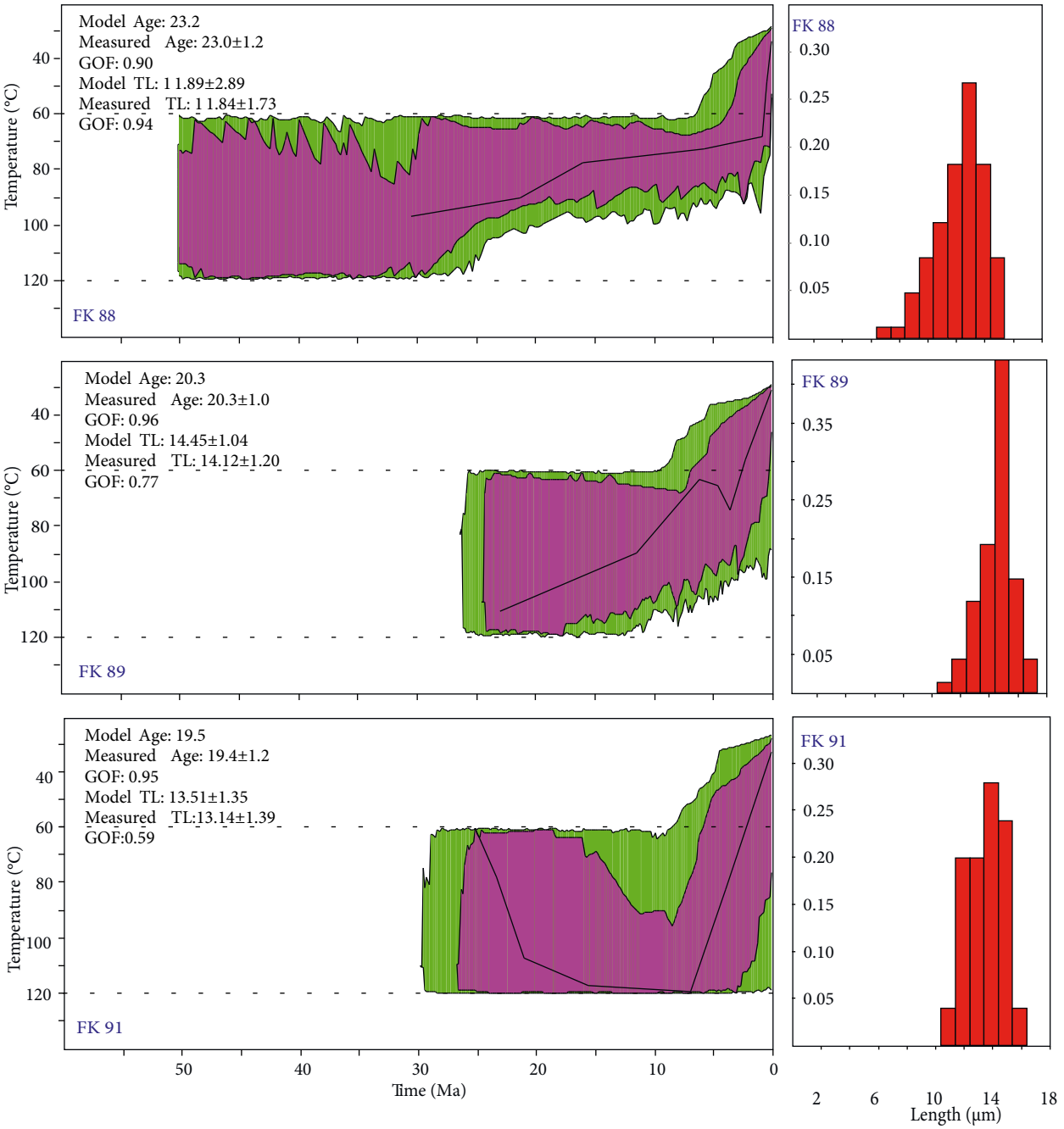

Figure 5. On the left, the time-temperature (T-t) paths for samples FK88, FK89, and FK91 modeled by HeFTy (Ketcham, 2005) using a Monte Carlo algorithm are shown. The software plots envelopes in a T-t space from the paths, for which all statistical parameters of the models are either greater than 0.50, corresponding to "good" (purple area) fit, or above 0.05, corresponding to "acceptable" (green area) fit. The solid black line shows the best-fit curve. On the right, the measured track-length distributions are shown. 'Model Age' is the fission-track age predicted by HeFTy. 'Measured Age' is the pooled age from the measured data. 'Model TL' is the mean and standard deviation of the track-length distribution predicted by HeFTy. 'Measured TL' is the mean and standard deviation of the measured track length distribution. 'GOF' defines the value of the goodness-of-fit between the model and measured ages and length distribution.

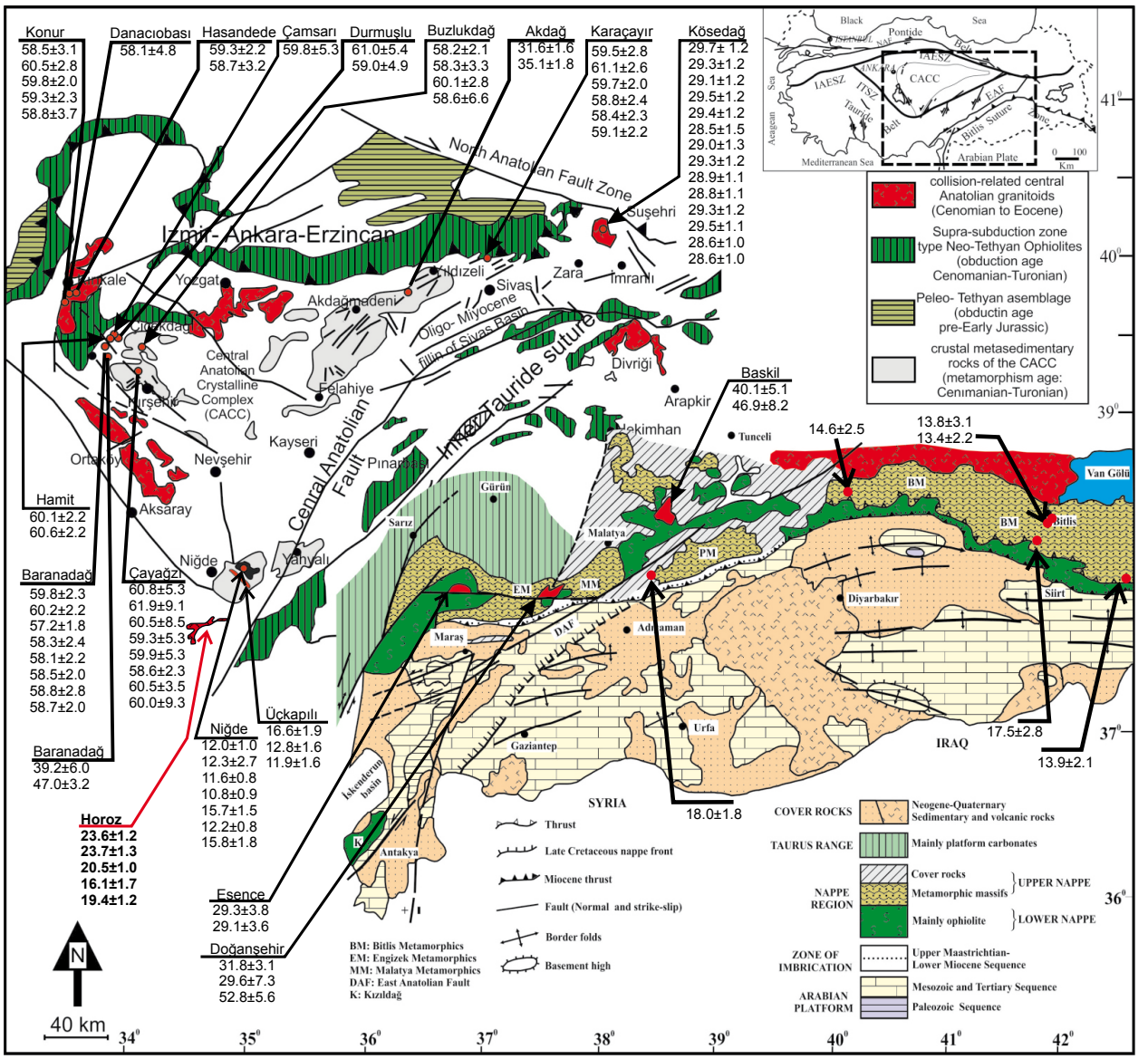

Figure 6. AFT age data from central and southeast Turkey. Inset map: Turkey, with dashed line box showing the outer map (map data from Yılmaz, 1993; Boztuğ et al., 2004, 2009b and AFT data from Dilek et al., 1999b; Fayon et al., 2001; Boztuğ et al., 2004, 2008, 2009a, 2009b, 2009c; Boztuğ and Jonckheere, 2007; Umhoefer et al., 2007; Okay et al., 2010; Karaoğlan, 2012).

remained active to recent times (Toprak and Göncüoğlu, 1993; Tatar et al., 2000; Jaffey and Robertson, 2001, 2005; Gautier et al., 2002). After the formation of the Ulukışla Basin, the Niğde Massif units experienced a burial event starting at the Middle Eocene, which raised temperatures to over 120 °C, causing a resetting of AFT ages (Whitney et al., 2003, 2008; Fayon and Whitney, 2007) (Figure 6). The Anatolide-Tauride platform underwent an extensional collapse during the Oligocene-Miocene. South-central Anatolia emerged above sea level during the Oligocene, as demonstrated by the deposition of Oligocene terrestrial sediments in the Ulukışla Basin between the CACC and Bolkar Mountains, Ecemiş Fault Zone, and Karsantı Basin in the east, and the Bucakkışla region in the west and Mut Basin and Adana Basin in the south (Yetiş and Demirkol, 1986; Görür, 1992; Dilek et al., 1999b; Clark and Robertson, 2002, 2005; Jaffey and Robertson, 2005; Şafak et al., 2005; Alan et al., 2007; Derman and Gürbüz, 2007; Cosentino et al., 2012; Esirtgen, 2014). Following the emergence, the ophiolitic rocks, which were emplaced onto the Bolkar Mountains during the Late Cretaceous, eroded in the first order and fed the adjacent basins (i.e. Ecemiş Basin) (Jaffey and Robertson, 2001, 2005). Braided rivers transported the ophiolitic sediments to the Oligocene-Early Miocene

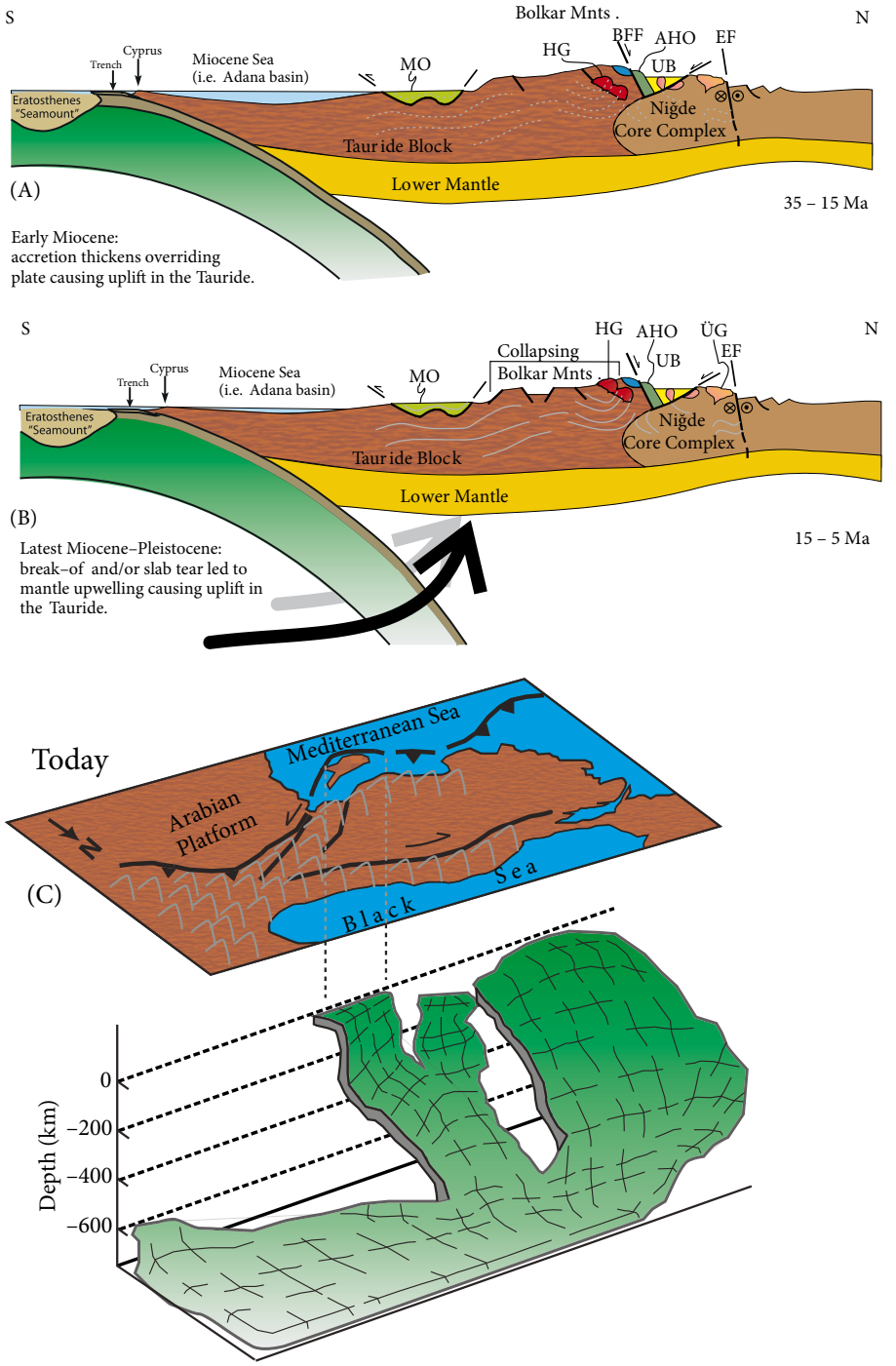

Figure 7. A) The geodynamic model of south-central Anatolia during the Oligo-Miocene. B) Geodynamic model of south-central Anatolia during the Latest Miocene-Pleistocene (data from Dilek and Whitney, 1997; Fayon and Whitney, 2007; Whitney et al., 2008; Kadıoğlu and Dilek, 2010). C) Today's mantle conditions beneath Anatolia. The slab break-off initiated beneath eastern Anatolia during the Oligocene and propagated toward the west. During the Latest Miocene, combination with slab-tear led to asthenospheric upwelling beneath south-central Anatolia, causing uplift in the region (Biryol et al., 2011; van Hunen and Allen, 2011; Cosentino et al., 2012; Schildgen et al., 2012a, 2012b, 2014) (MO: Mersin Ophiolite, HG: Horozköy Granitoid, BFF: Bolkar Frontal Fault, AHO: Ali Hoca Ophiolite, UB: Ulukışla Basin, EF: Ecemiş Fault, ÜG: Üçkapılı Granitoid). A and B modified after Kadıoğlu and Dilek (2010), C modified after Schildgen et al. (2014).

basins. During the early-middle Miocene, the Niğde Massif and the Bolkar Mountains were uplifted as a result of mantle processes (slab-rollback, slab break-off, and/or slab tear) beneath south-central Anatolia and fed the adjacent basins (Şengör and Yılmaz, 1981; Jaffey and Robertson, 2005; Biryol et al., 2011; Cosentino et al., 2012; Robertson et al., 2012; Schildgen et al., 2012a, 2012b, 2014) (Figure 7). Western Anatolia and the Aegean region, similar to the Bolkar Mountains, experienced a limited exhumation of the metamorphic rocks along the margins and the opening of the Aegean Sea Basin during the early Miocene (Ring et al., 2010). To the north of the Bolkar Mountains, the Niğde Massif was exhumed as result of strike-slip faulting in a yo-yo tectonic regime with a high rate (>1 mm/year) between 20 and 10 Ma (Fayon et al., 2001; Fayon and Whitney, 2007; Umhoefer et al., 2007; Whitney et al., 2008). To the south of the Bolkar Mountains, the island of Cyprus was already uplifted above sea level during the Miocene (Robertson, 1977, 2002, 2012; Kinnaird et al., 2011). Besides the fast exhumation of the Niğde Massif during the Early Miocene, the Bolkar Mountains were exhumed very slowly (<0.5 mm/year) during this period (Figures 4–6). The Bolkar Mountains may have been shaped by erosion during this stage; however, the paleogeothermal gradient was high enough that the AFT data do not record an important exhumation phase (Figure 5). While the compressional events were responsible for the Oligo-Miocene slow uplift of the region, multiple sources such as slab break-off, slab tearing, and/or collision of a continental fragment with the subduction zone south of Cyprus were uplifted in the region with high uplift rates during the latest Miocene-Pleistocene (Cosentino et al., 2012; Schildgen et al., 2012a, 2012b, 2014). The Bolkar Mountains reached their maximum elevation by 8–5 Ma, as a result of continued crustal uplift along the Bolkar Frontal Fault (Dilek et al., 1999b; Schildgen et al., 2012a, 2014). The fast erosion of the Bolkar and Aladağ mountains, related to the mantle processes, caused uplifting of this region as high as ~2000–3000 m, where the Horozköy granitoid outcropped during 15–5 Ma and the sediments from the Horozköy granitoid were transported to the adjacent terrestrial and marine environment (i.e. Adana Basin, south of the Bolkar Mountains) by the late Miocene (Gürbüz, 1993; Gürbüz and Kelling, 1993; Jaffey and Robertson, 2005; Ilgar et al., 2013). Recent studies showed that the uplift of the Central Taurides started at 7–8 Ma and since that time the marine sedimentary units uplifted ~2 km high in the region, which is consistent with a fast cooling profile as constrained by the AFT data obtained in this study (Cosentino et al., 2012; Schildgen et al., 2012a, 2012b, 2014; Cipollari et al., 2013; Radeff et al., 2015).

6. Conclusion

Suturing of the ITSZ and the juxtaposition of the CACC and Central Taurides caused folding, thrusting, and regional emergence above eustatic sea level and ended the Tethys-related marine sedimentation in the Central Taurus in Late Eocene time. The uplifting of the Central Taurides during the late Tertiary was closely associated with mountain-building processes in a collided continental collision zone. The collision of Africa-Arabia to the south and Eurasia to the north caused high uplift in eastern Anatolia, whereas the Anatolide-Tauride platform underwent an extensional collapse during the Oligocene-early Miocene (Şengör and Yılmaz, 1981; Şengör, 1985; Şengör et al., 1985, 2003; Dewey et al., 1986; Jolivet and Faccenna, 2000; Aksu et al., 2005b; Bozkurt and Mittwede, 2005; Ring et al., 2010; Elitok and Dolmaz, 2011). The late Miocene of the region witnessed a high uplift of the mountain belt and subsidence in the foreland as a result of the slab break-off and/or the slab tear within the subducted slab beneath this region (Cosentino et al., 2012; Schildgen et al., 2012a, 2012b, 2014; Cipollari et al., 2013) (Figure 7).

The AFT data obtained in this study suggest:

1) The Horozköy granitoid was emplaced in a shallow depth and reached 2–3 km in depth corresponding to the PAZ of AFTs during the early-middle Miocene. This period was most likely vertically stable in the region such that the Horozköy granitoid was exhumed very slowly (<<0.5 mm/year) and remained in the PAZ (2–3 km in depth) until ~10 Ma.
2) After ~10 Ma, during the late Miocene-early Pleistocene, the region uplifted very fast together with the unroofing of the Horozköy granitoid (>1 mm/year), as a result of slab break-off and slab tearing of the oceanic lithosphere linked to the African plate beneath south-central Anatolia, which is consistent with biostratigraphic and field evidence from the Oligocene terrestrial and Miocene marine and terrestrial sediments.

Acknowledgments

The author acknowledges Taylor F Schildgen and two anonymous reviewers, as well as Associate Editor M Cemal Göncüoğlu, for providing detailed and constructive reviews that helped to improve the manuscript. This work was supported by the Research Fund of Çukurova University (FBA-2015-3652) and TÜBİTAK (Project no: 112Y347). The author was financially supported by the Research Fund of Çukurova University (FBI-2014-2742).

References

Aksu AE, Calon TJ, Hall J, Mansfield S, Yaşar D (2005a). The Cilicia–Adana basin complex, Eastern Mediterranean: Neogene evolution of an active fore-arc basin in an obliquely convergent margin. Mar Geol 221: 121–159.

Aksu AE, Hall J, Yaltırak C (2005b). Miocene to Recent tectonic evolution of the eastern Mediterranean: new pieces of the old Mediterranean puzzle. Mar Geol 221: 1–13.

Alan İ, Şahin Ş, Keskin H, Altun İ, Bakirhan B, Balci V, Böke N, Saçlı L, Pehlivan Ş, Kop A et al. (2007). Orta Toroslar'ın Jeodinamik Evrimi Ereğli (Konya)-Ulukışla (Niğde)-Karsantı (Adana)-Namrun (İçel) Yöresi. Ankara, Turkey: Maden Tetkik ve Arama Genel Müdürlüğü (in Turkish).

Allen MB, Armstrong HA (2008). Arabia-Eurasia collision and the forcing of mid-Cenozoic global cooling. Palaeogeogr Palaeocl 265: 52–58.

Balestrieri ML, Bernet M, Brandon MT, Picotti V, Reiners P, Zattin M (2003). Pliocene and Pleistocene exhumation and uplift of two key areas of the Northern Apennines. Quatern Int 101–102: 67–73.

Barazangi M, Sandvol E, Seber D (2006). Structure and tectonic evolution of the Anatolian plateau in eastern Turkey. In: Dilek, Y, Pavlides, S editors. Postcollisional Tectonics and Magmatism in the Mediterranean Region and Asia. Geological Society of America Special Papers, Vol. 409. Boulder, CO, USA: GSA, pp. 463–473.

Biryol CB, Beck SL, Zandt G, Özacar AA (2011). Segmented African lithosphere beneath the Anatolian region inferred from teleseismic P-wave tomography. Geophys J Int 184: 1037–1057.

Blumenthal M (1956). Yüksek Bolkardağın kuzey kenar bölgelerinin ve batı uzantılarının jeolojisi. Ankara, Turkey: MTA (in Turkish).

Blumenthal M (1960). Le système structural du Taurus sud-anatolien. Livre à la mémoire du Professeur P. Fallot. Mémoires de la Société géologique de France 2: 661–662 (in French).

Bozkurt E, Mittwede SK (2005). Introduction: Evolution of continental extensional tectonics of western Turkey. Geodin Acta 18: 153–165.

Boztuğ D, Güney Ö, Heizler M, Jonckheer RJ, Tichomirowa M, Otlu N (2009a). ^{207}Pb-^{206}Pb, ^{40}Ar-^{39}Ar and fission-track geothermochronology quantifying cooling and exhumation history of the Kaman-Kırşehir Region intrusions, Central Anatolia, Turkey. Turk J Earth Sci 18: 85–108.

Boztuğ D, Jonckheere R, Wagner GA, Yegingil Z (2004). Slow Senonian and fast Palaeocene-Early Eocene uplift of the granitoids in the Central Eastern Pontides, Turkey: apatite fission-track results. Tectonophysics 382: 213–228.

Boztuğ D, Jonckheere RC (2007). Apatite fission track data from central Anatolian granitoids (Turkey): constraints on Neo-Tethyan closure. Tectonics 26: TC3011.

Boztuğ D, Jonckheere RC, Heizler M, Ratschbacher L, Harlavan Y, Tichomirova M (2009b). Timing of post-obduction granitoids from intrusion through cooling to exhumation in central Anatolia, Turkey. Tectonophysics 473: 223–233.

Boztuğ D, Temiz H, Jonckheere R, Ratschbacher L (2008). Punctuated exhumation and foreland basin formation and infilling in (circum)-Central Anatolia (Turkey) associated with the Neo-Tethyan closure. Turk J Earth Sci 17: 673–684.

Boztuğ D, Türksever E, Heizler M, Jonckheere R, Tichomirowa M (2009c). ^{207}Pb-^{206}Pb, ^{40}Ar-^{39}Ar and Apatite Fission-Track Geothermochronology Revealing the Emplacement, Cooling and Exhumation History of the Karacayir Syenite (N Sivas), East-Central Anatolia, Turkey. Turk J Earth Sci 18: 109–125.

Çalapkulu F (1980). Horoz Granodiyoritinin Jeolojik incelemesi. Türkiye Jeoloji Bülteni 23: 59–69 (in Turkish).

Çevikbaş A, Boztuğ D, Demirkol C, Yılmaz S, Akyıldız M, Açlan M, Demir Ö, Taş R (1995). Horoz Plütonun (Ulukışla - Niğde) oluşumunda dengelenmiş hibrid sistemin minerolojik ve jeokimyasal kanıtları. Türkiye Jeoloji Kurultayı Bülteni 10: 62–67 (in Turkish).

Çevikbaş A, Öztunalı Ö (1992). Ulukışla-Çamardı (Niğde) Mestrihtiyen sonrası gölsel havzasının jeolojisi. Maden Tetkik ve Arama Enstitüsü Dergisi 114: 155–172 (in Turkish).

Cipollari P, Cosentino D, Radeff G, Schildgen TF, Faranda C, Grossi F, Gliozzi E, Smedile A, Gennari R, Darbaş G et al. (2013). Easternmost Mediterranean evidence of the Zanclean flooding event and subsequent surface uplift: Adana Basin, southern Turkey. In: Robertson AHF, Parlak O, Ünlügenç UC, editors. Geological Development of Anatolia and the Easternmost Mediterranean Region. Special Publication Vol. 372. London, UK: The Geological Society, pp. 473–494.

Clark M, Robertson A (2002). The role of the Early Tertiary Ulukisla Basin, southern Turkey, in suturing of the Mesozoic Tethys ocean. J Geol Soc London 159: 673–690.

Clark M, Robertson AHF (2005). Uppermost Cretaceous–Lower Tertiary Ulukışla Basin, south-central Turkey: sedimentary evolution of part of a unified basin complex within an evolving Neotethyan suture zone. Sediment Geol 173: 15–51.

Cosentino D, Schildgen TF, Cipollari P, Faranda C, Gliozzi E, Hudáčková N, Lucifora S, Strecker MR (2012). Late Miocene surface uplift of the southern margin of the Central Anatolian Plateau, Central Taurides, Turkey. Geol Soc Am Bull 124: 133–145.

Demirtaşlı E, Bilgin AZ, Erenler F, Işıklar S, Sanlı DY, Selim M, Turhan N (1973). Bolkardağları'nın Jeolojisi. In: Cumhuriyetin 50. Yılı Kongresi, pp. 42–57 (in Turkish).

Demirtaşlı E, Turhan N, Bilgin AZ, Selim M (1984). Geology of the Bolkar Mountains. In: Tekeli O, Göncüoğlu MC, editors. Geology of the Taurus Belt. Ankara, Turkey: Mineral Research and Exploration Institute of Turkey, pp. 125–141.

Derman AS, Gürbüz K (2007). Nature, provenance and relationships of early Miocene palaeovalley fills, northern Adana Basin, Turkey: their significance for sediment-bypassing on a carbonate shelf. Turk J Earth Sci 16: 181-209.

Dewey JF, Hempton MR, Kidd WSF, Saroglu F, Şengör AMC (1986). Shortening of continental lithosphere: the neotectonics of Eastern Anatolia — a young collision zone. In: Coward MP, Ries AC, editors. Collision Tectonics. Special Publication Vol. 19. London, UK: The Geological Society, pp. 1–36.

Dilek Y, Flower MFJ (2003). Arc-trench rollback and forearc accretion: 2. A model template for ophiolites in Albania, Cyprus, and Oman. In: Dilek Y, Robinson PT, editors. Ophiolites in Earth History. Special Publication Vol. 218. London, UK: The Geological Society, pp. 43–68.

Dilek Y, Sandvol E (2009). Seismic structure, crustal architecture and tectonic evolution of the Anatolian-African Plate Boundary and the Cenozoic Orogenic Belts in the Eastern Mediterranean Region. In: Murphy JB, Keppie JD, Hynes AJ, editors. Ancient Orogens and Modern Analogues. Special Publication Vol. 327. London, UK: The Geological Society, pp. 127–160.

Dilek Y, Thy P, Hacker B, Grundvig S (1999a). Structure and petrology of Tauride ophiolites and mafic dike intrusions (Turkey): implications for the Neotethyan ocean. Geol Soc Am Bull 111: 1192–1216.

Dilek Y, Whitney DL (1997). Counterclockwise P-T-t trajectory from the metamorphic sole of a Neo-Tethyan ophiolite (Turkey). Tectonophysics 280: 295–310.

Dilek Y, Whitney DL (2000). Cenozoic crustal evolution in Central Anatolia: extension, magmatism and landscape development. In: Panayides I, Xenophontos C, Malpas J, editors. Proceedings of the Third International Conference on the Geology of the Eastern Mediterranean, pp. 183–192.

Dilek Y, Whitney DL, Tekeli O (1999b). Links between neotectonic processes and landscape evolution in an Alpine collision zone, south-central Turkey. Zeitschrift fur Geomorphologie Supplement 118: 147–164.

Donelick RA, Ketcham RA, Carlson WD (1999). Variability of apatite fission-track annealing kinetics: II. Crystallographic orientation effects. Am Mineral 84: 1224–1234.

Elitok Ö, Dolmaz MN (2011). Tectonic escape mechanism in the crustal evolution of Eastern Anatolian Region (Turkey). In: Schattner U, editor. New Frontiers in Tectonic Research - At the Midst of Plate Convergence. Rijeka, Croatia: InTech, pp. 289–302.

Engin C (2013). Structural architecture and tectonic evolution of the Ulukisla Sedimentary Basin in south-central Turkey. MSc, Miami University, Oxford, OH, USA.

Esirtgen T (2014). Tectono - sedimentary evolution of Bucakkıışla Region (SW Karaman) in Central Taurides. Bulletin of Mineral Research and Exploration 148: 19–42.

Fayon AK, Whitney DL (2007). Interpretation of tectonic versus magmatic processes for resetting apatite fission track ages in the Nigde Massif, Turkey. Tectonophysics 434: 1–13.

Fayon AK, Whitney DL, Teyssier C, Garver JI, Dilek Y (2001). Effects of plate convergence obliquity on timing and mechanisms of exhumation of a mid-crustal terrain, the Central Anatolian Crystalline Complex. Earth Planet Sc Lett 192: 191–205.

Galbraith RF, Laslett GM (1993). Statistical models for mixed fission track ages. Nucl Tracks Rad Meas 21: 459–470.

Gallagher K, Brown R, Johnson C (1998). Fission track analysis and its applications to geological problems. Annu Rev Earth Pl Sc 26: 519–572.

Gallagher K, Stephenson J, Brown R, Holmes C, Fitzgerald P (2005). Low temperature thermochronology and modeling strategies for multiple samples 1: Vertical profiles. Earth Planet Sc Lett 237: 193–208.

Garfunkel Z (1998). Constrains on the origin and history of the Eastern Mediterranean basin. Tectonophysics 298: 5–35.

Garfunkel Z (2004). Origin of the Eastern Mediterranean basin: a reevaluation. Tectonophysics 391: 11–34.

Gautier P, Bozkurt E, Hallot E, Dirik K (2002). Dating the exhumation of a metamorphic dome: geological evidence for pre-Eocene unroofing of the Niğde Massif (Central Anatolia, Turkey). Geol Mag 139: 559–576.

Gleadow AJW, Lovering JF (1977). Geometry factor for external detectors in fission track dating. Nuclear Track Detection 1: 99–106.

Göncüoğlu C (1986). Geochronologic data from the southern part (Niğde area) of the Central Anatolian Massif. Maden Tetkik ve Arama Dergisi 105/106: 83–96.

Göncüoğlu MC, Toprak V, Kuşcu İ, Erler A, Olgun E (1991). Geology of the Western Part of the Central Anatolian Massif, Part 1: Southern Section. Ankara, Turkey: Turkish Petroleum Company.

Görür N (1992). A tectonically controlled alluvial-fan which developed into a marine fan-delta at a complex triple junction - Miocene-Gildirli Formation of the Adana Basin, Turkey. Sediment Geol 81: 243–252.

Görür N, Oktay FY, Seymen İ, Şengör AMC (1984). Palaeotectonic evolution of the Tuzgölü basin complex, Central Turkey: sedimentary record of a Neo-Tethyan closure. In: Dixon JE, Robertson AHF, editors. The Geological Evolution of the Eastern Mediterranean. Special Publication Vol. 17. London, UK: The Geological Society, pp. 467–482.

Görür N, Şengör AMC, Sakınç M, Tüysüz O, Yiğitbaş E, Oktay FY, Engin S, Okuroğulları AH, Özgül K (1991). Türkiye ve çevresinin Geç Triyas-Geç Miyosen Dönemindeki paleocografik evrimi. In: Ozan Sungurlu Sempozyumu, pp. 174–189 (in Turkish).

Gürbüz K (1993). Identification and evolution of Miocene submarine fans in the Adana Basin, Turkey. PhD, University of Keele, Keele, UK.

Gürbüz K, Kelling G (1993). Provenance of Miocene submarine fans in the northern Adana Basin: a test of discriminant function analysis. Geol J 28: 277–295.

Ilgar A, Nemec W, Hakyemez A, Karakuş E (2013). Messinian forced regressions in the Adana Basin: a near-coincidence of tectonic and eustatic forcing. Turk J Earth Sci 22: 864–889.

Jaffey N, Robertson AHF (2001). New sedimentological and structural data from the Ecemis Fault Zone, southern Turkey: implications for its timing and offset and the Cenozoic tectonic escape of Anatolia. J Geol Soc London 158: 367–378.

Jaffey N, Robertson AHF (2005). Non-marine sedimentation associated with Oligocene-Recent exhumation and uplift of the Central Taurus Mountains, S Turkey. Sediment Geol 173: 53–89.

Jarvis A, Reuter HI, Nelson A, Guevara E (2008). Hole-filled seamless SRTM data V4. Cali, Columbia: International Center for Tropical Agriculture (CIAT). Available online at http://srtm.csi.cgiar.org.

Jolivet L, Faccenna C (2000). Mediterranean extension and the Africa-Eurasia collision. Tectonics 19: 1095–1106.

Jonckheere R, Ratschbacher L, Wagner GA (2003). A repositioning technique for counting induced fission tracks in muscovite external detectors in single-grain dating of minerals with low and inhomogeneous uranium concentrations. Radiat Meas 37: 217–219.

Kadıoğlu YK, Dilek Y (2010). Structure and geochemistry of the adakitic Horoz granitoid, Bolkar Mountains, south-central Turkey, and its tectonomagmatic evolution. Int Geol Rev 52: 505–535.

Kadıoğlu YK, Dilek Y, Foland KA (2006). Slab break-off and syncollisional origin of the Late Cretaceous magmatism in the Central Anatolian crystalline complex, Turkey. In: Dilek Y, Pavlides S, editors. Postcollisional Tectonics and Magmatism in the Mediterranean Region and Asia. Geological Society of America Special Papers, Vol. 409. Boulder, CO, USA: GSA, pp. 381–415.

Karaoğlan F (2012). Güneydoğu Anadolu orojenik kuşağindaki ofiyolitik ve granitik kayaçların jeokronolojisi. PhD, Çukurova University, Adana, Turkey (in Turkish).

Karaoğlan F, Parlak O, Hejl E, Neubauer F, Klötzli U (2015). The temporal evolution of the active margin along the Southeast Anatolian Orogenic Belt (SE Turkey): evidence from U-Pb, Ar-Ar and fission track chronology. Gondwana Res (in press).

Ketcham RA (2005). Forward and inverse modeling of low-temperature thermochronometry data. In: Reiners PW, Ehlers TA, editors. Low-Temperature Thermochronology: Techniques, Interpretations, and Applications. Vol. 58. Chantilly, VA, USA: Mineralogical Society of America, pp. 275–314.

Kinnaird TC, Robertson AHF, Morris A (2011). Timing of uplift of the Troodos Massif (Cyprus) constrained by sedimentary and magnetic polarity evidence. J Geol Soc London 168: 457–470.

Kocak K, Zedef V, Kansun G (2011). Magma mixing/mingling in the Eocene Horoz (Nigde) granitoids, Central southern Turkey: evidence from mafic microgranular enclaves. Miner Petrol 103: 149–167.

Kurt MA, Alpaslan M, Göncüoğlu MC, Temel A (2008). Geochemistry of late stage medium to high-K calc-alkaline and shoshonitic dykes in the Ulukişla Basin (Central Anatolia, Turkey): petrogenesis and tectonic setting. Geochem Int+ 46: 1145–1163.

Kuscu I, Kuscu GG, Tosdal RM, Ulrich TD, Friedman R (2010). Magmatism in the southeastern Anatolian orogenic belt: transition from arc to post-collisional setting in an evolving orogen. Geol Soc Sp 340: 437–460.

Lefebvre C, Thomson SN, Reiners PW, Whitney DL, Teyssier C (2015). Thermochronologic evaluation of the Arabia-Anatolia collision: new results from apatite (U-Th)He and fission track. In: EGU2015, p. EGU2015-7623.

McClusky S, Balassanian S, Barka A, Demir C, Ergintav S, Georgiev I, Gurkan O, Hamburger M, Hurst K, Kahle H et al. (2000). Global Positioning System constraints on plate kinematics and dynamics in the eastern Mediterranean and Caucasus. J Geophys Res-Sol Ea 105: 5695–5719.

McDougall I, Harrison TM (1999). Geochronology and Thermochronology by the $^{40}Ar/^{39}Ar$ Method. 2nd ed. New York, NY, USA: Oxford University Press.

Okay AI, Tüysüz O (1999). Tethyan sutures of northern Turkey. In: Durand B, Jolivet FL, Horváth F, editors. The Mediterranean Basins: Tertiary Extension within the Alpine Orogen. Special Publication Vol. 156. London, UK: The Geological Society, pp. 475–515.

Okay AI, Zattin M, Cavazza W (2010). Apatite fission-track data for the Miocene Arabia-Eurasia collision. Geology 38: 35–38.

Özgül N (1976). Toroslar'ın bazı temel jeoloji özellikleri. Türkiye Jeoloji Bülteni 19: 65–78.

Özgül N (1984). Stratigraphy and tectonic evolution of the Central Taurides. In: Tekeli O, Göncüoğlu MC, editors. Geology of the Taurus Belt. Ankara, Turkey: Mineral Research and Exploration Institute of Turkey, pp. 77–90.

Parlak O, Karaoğlan F, Rızaoğlu T, Klötzli U, Koller F, Billor Z (2013). U–Pb and $^{40}Ar–^{39}Ar$ geochronology of the ophiolites and granitoids from the Tauride belt: implications for the evolution of the Inner Tauride suture. J Geodyn 65: 22–37.

Parlak O, Kop A, Robertson AHF, Karaoğlan F, Neubauer F, Köpke J (2014). Upper Cretaceous HP-LT metamorphism along the leading edge of the Mesozoic Bolkardag Platform, Southern Turkey. In: European Geosciences Union General Assembly 2014 (EGU2014), p. EGU2014-3665-2012.

Parlak O, Robertson A (2004). The ophiolite-related Mersin Melange, southern Turkey: its role in the tectonic-sedimentary setting of Tethys in the Eastern Mediterranean Region. Geol Mag 141: 257–286.

Pourteau A (2011). Closure of the Neotethys Ocean in Anatolia: structural, petrologic & geochronologic insights from low-grade high-pressure metasediments, Afyon Zone. PhD, University of Potsdam, Potsdam, Germany.

Pourteau A, Bousquet R, Vidal O, Plunder A, Duesterhoeft E, Candan O, Oberhänsli R (2014). Multistage growth of Fe–Mg–carpholite and Fe–Mg–chloritoid, from field evidence to thermodynamic modelling. Contrib Mineral Petr 168: 1–25.

Pourteau A, Candan O, Oberhänsli R (2010). High-pressure metasediments in central Turkey: Constraints on the Neotethyan closure history. Tectonics 29: TC5004.

Pourteau A, Sudo M, Candan O, Lanari P, Vidal O, Oberhansli R (2013). Neotethys closure history of Anatolia: insights from Ar-40-Ar-39 geochronology and P-T estimation in high-pressure metasedimentary rocks. J Metamorph Geol 31: 585–606.

Radeff G, Schildgen TF, Cosentino D, Strecker MR, Cipollari P, Darbaş G, Gürbüz K (2015). Sedimentary evidence for late Messinian uplift of the SE margin of the Central Anatolian Plateau: Adana Basin, southern Turkey. Basin Res (in press).

Reilinger RE, McClusky SC, Oral MB, King RW, Toksoz MN, Barka AA, Kinik I, Lenk O, Sanli I (1997). Global Positioning System measurements of present-day crustal movements in the Arabia-Africa-Eurasia plate collision zone. J Geophys Res-Sol Ea 102: 9983–9999.

Ring U, Glodny J, Will T, Thomson S (2010). The Hellenic Subduction System: high-pressure metamorphism, exhumation, normal faulting, and large-scale extension. Annu Rev Earth Pl Sc 38: 45–76.

Robertson AHF (1977). Tertiary uplift history of the Troodos massif, Cyprus. Geol Soc Am Bull 88: 1763–1772.

Robertson AHF (2002). Overview of the genesis and emplacement of Mesozoic ophiolites in the Eastern Mediterranean Tethyan region. Lithos 65: 1–67.

Robertson AHF (2004). Development of concepts concerning the genesis and emplacement of Tethyan ophiolites in the Eastern Mediterranean and Oman regions. Earth-Sci Rev 66: 331–387.

Robertson AHF, Dixon JE (1984). Introduction: Aspects of the geological evolution of the Eastern Mediterranean. In: Robertson AHF, Dixon JE, editors. The Geological Evolution of the Eastern Mediterranean. Special Publication Vol. 17. London, UK: The Geological Society, pp. 1–74.

Robertson AHF, Mountrakis D (2006). Tectonic development of the Eastern Mediterranean region: an introduction. In: Robertson AHF, Mountrakis D, editors. Tectonic Development of the Eastern Mediterranean Region. Special Publication Vol. 260. London, UK: The Geological Society, pp. 1–9.

Robertson AHF, Parlak O, Ustaomer T (2012). Overview of the Palaeozoic-Neogene evolution of Neotethys in the Eastern Mediterranean region (Southern Turkey, Cyprus, Syria). Petrol Geosci 18: 381–404.

Şafak Ü, Kelling G, Gökçen NS, Gürbüz K (2005). The mid-Cenozoic succession and evolution of the Mut basin, southern Turkey, and its regional significance. Sediment Geol 173: 121–150.

Sarıfakıoğlu E, Dilek Y, Winchester JA (2013). Late Cretaceous subduction initiation and Palaeocene-Eocene slab breakoff magmatism in South-Central Anatolia, Turkey. Int Geol Rev 55: 66–87.

Schildgen TF, Cosentino D, Bookhagen B, Niedermann S, Yildirim C, Echtler H, Wittmann H, Strecker MR (2012a). Multi-phased uplift of the southern margin of the Central Anatolian plateau, Turkey: a record of tectonic and upper mantle processes. Earth Planet Sc Lett 317: 85–95.

Schildgen TF, Cosentino D, Caruso A, Buchwaldt R, Yildirim C, Bowring SA, Rojay B, Echtler H, Strecker MR (2012b). Surface expression of eastern Mediterranean slab dynamics: Neogene topographic and structural evolution of the southwest margin of the Central Anatolian Plateau, Turkey. Tectonics 31: TC2005.

Schildgen TF, Yildirim C, Cosentino D, Strecker MR (2014). Linking slab break-off, Hellenic trench retreat, and uplift of the Central and Eastern Anatolian plateaus. Earth-Sci Rev 128: 147–168.

Şengör AMC (1985). Türkiye'nin tektonik tarihinin yapısal sınıflaması. In: Ketin Simpozyumu Kitabı, pp. 37–62 (in Turkish).

Şengör AMC, Gorur N, Şaroğlu F (1985). Strike-slip faulting and related basin formation in zones of tectonic escape: Turkey as a case study. In: Biddle KT, Christie-Blick N, editors. Strike-Slip Deformation, Basin Formation, and Sedimentation. Special Publication Vol. 37. Tulsa, OK, USA: Society of Economic Paleontologists and Mineralogists, pp. 227–264.

Şengör AMC, Özeren S, Genç T, Zor E (2003). East Anatolian high plateau as a mantle-supported, north-south shortened domal structure. Geophys Res Lett 30: 8045.

Şengör AMC, Yılmaz Y (1981). Tethyan Evolution of Turkey - a Plate Tectonic Approach. Tectonophysics 75: 181-241.

Smith AG (2006). Tethyan ophiolite emplacement, Africa to Europe motions, and Atlantic spreading. In: Robertson AHF, Mountrakis D, editors. Tectonic Development of the Eastern Mediterranean Region. Special Publication Vol. 260. London, UK: The Geological Society, pp. 11–34.

Tatar O, Piper JDA, Gürsoy H (2000). Palaeomagnetic study of the Erciyes Sector of the Ecemiş Fault Zone: neotectonic deformation in the southeastern part of the Anatolian Block. In: Bozkurt E, Winchester JA, Piper JA, editors. Tectonics and Magmatism in Turkey and the Surrounding Area. Special Publication Vol. 173. London, UK: The Geological Society, pp. 423–440.

Tezel T, Shibutani T, Kaypak B (2013). Crustal thickness of Turkey determined by receiver function. J Asian Earth Sci 75: 36–45.

Toprak V, Göncüoğlu MC (1993). Tectonic control on the development of the Neogene Quaternary Central Anatolian Volcanic Province, Turkey. Geol J 28: 357–369.

Umhoefer PJ, Whitney DL, Teyssier C, Fayon AK, Casale G, Heizler MT (2007). Yo-yo tectonics in a wrench zone, Central Anatolian fault zone, Turkey. Geol S Am S 434: 35–57.

Van Den Haute P, De Corte F (editors) (1998). Advances in Fission-Track Geochronology. Amsterdam, the Netherlands: Springer.

Van Hinsbergen DJJ, Edwards MA, Govers R (2009). Geodynamics of collision and collapse at the Africa-Arabia-Eurasia subduction zone – an introduction. In: Van Hinsbergen DJJ, Edwards MA, Govers R, editors. Collision and Collapse at the Africa-Arabia-Eurasia Subduction Zone. Special Publication Vol. 311. London, UK: The Geological Society, pp. 1–7.

Van Hunen J, Allen MB (2011). Continental collision and slab break-off: a comparison of 3-D numerical models with observations. Earth Planet Sc Lett 302: 27–37.

Wagner GA, Van den Haute P (1992). Fission Track-Dating. Dordrecht, the Netherlands: Kluwer Academic Publishers.

Whitney DL, Dilek Y (1997). Core complex development in central Anatolia, Turkey. Geology 25: 1023–1026.

Whitney DL, Dilek Y (1998). Metamorphism during alpine crustal thickening and extension in Central Anatolia, Turkey: the Niğde Metamorphic Core Complex. J Petrol 39: 1385–1403.

Whitney DL, Dilek Y (2000). Andalusite-sillimanite-quartz veins as indicators of low-pressure-high-temperature deformation during late-stage unroofing of a metamorphic core complex, Turkey. J Metamorph Geol 18: 59–66.

Whitney DL, Teyssier C, Dilek Y, Fayon AK (2001). Metamorphism of the Central Anatolian Crystalline Complex, Turkey: influence of orogen-normal collision vs. wrench-dominated tectonics on P-T-t paths. J Metamorph Geol 19: 411–432.

Whitney DL, Teyssier C, Fayon AK, Hamilton MA, Heizler M (2003). Tectonic controls on metamorphism, partial melting, and intrusion: timing and duration of regional metamorphism and magmatism in the Nigde Massif, Turkey. Tectonophysics 376: 37–60.

Whitney DL, Teyssier C, Heizler MT (2007). Gneiss domes, metamorphic core complexes, and wrench zones: thermal and structural evolution of the Niğde Massif, central Anatolia. Tectonics 26: TC5002.

Whitney DL, Umhoefer PJ, Teyssier C, Fayon AK (2008). Yo-yo tectonics of the Niğde Massif during wrenching in Central Anatolia. Turk J Earth Sci 17: 209–217.

Yetiş C, Demirkol C (1986). Adana Baseni Batı Kesiminin Detay Jeoloji Etüdü. Adana, Turkey: MTA Genel Müdürlüğü Jeoloji Etüdleri Dairesi (in Turkish).

Yildirim C, Melnick D, Ballato P, Schildgen TF, Echtler H, Erginal AE, Kıyak NG, Strecker MR (2013). Differential uplift along the northern margin of the Central Anatolian Plateau: inferences from marine terraces. Quaternary Sci Rev 81: 12–28.

Yılmaz H, Alpaslan M, Temel A (2007). Two-stage felsic volcanism in the western part of the southeastern Anatolian orogen: petrologic and geodynamic implications. Int Geol Rev 49: 120–141.

Yılmaz Y (1993). New evidence and model on the evolution of the Southeast Anatolian Orogen. Geol Soc Am Bull 105: 251–271.